The Borealin dimerization domain interacts with Sgo1 to drive Aurora B–mediated spindle assembly

Mary Kate Bonner[†], Julian Haase[†], Hayden Saunders[‡], Hindol Gupta, Biyun Iris Li[§], and Alexander E. Kelly*
Laboratory of Biochemistry and Molecular Biology, National Cancer Institute, NIH, Bethesda, MD 20892

ABSTRACT **The chromosomal passenger complex (CPC), which includes the kinase Aurora B, is a master regulator of meiotic and mitotic processes that ensure the equal segregation of chromosomes. Sgo1 is thought to play a major role in the recruitment of the CPC to chromosomes, but the molecular mechanism and contribution of Sgo1-dependent CPC recruitment is currently unclear. Using *Xenopus* egg extracts and biochemical reconstitution, we found that Sgo1 interacts directly with the dimerization domain of the CPC subunit Borealin. Borealin and the PP2A phosphatase complex can bind simultaneously to the coiled-coil domain of Sgo1, suggesting that Sgo1 can integrate Aurora B and PP2A activities to modulate Aurora B substrate phosphorylation. A Borealin mutant that specifically disrupts the Sgo1–Borealin interaction results in defects in CPC chromosomal recruitment and Aurora B–dependent spindle assembly, but not in spindle assembly checkpoint signaling at unattached kinetochores. These findings establish a direct molecular connection between Sgo1 and the CPC and have major implications for the different functions of Aurora B, which promote the proper interaction between spindle microtubules and chromosomes.**

Monitoring Editor
Kerry Bloom
University of North Carolina, Chapel Hill

Received: May 29, 2020
Revised: Jul 6, 2020
Accepted: Jul 13, 2020

INTRODUCTION

Accurate chromosome segregation during mitosis and meiosis depends on the spatiotemporal regulation of kinase and phosphatase activities (Ubersax and Ferrell, 2007). The kinase Aurora B, together with INCENP, Borealin, and Survivin, forms the chromosomal passenger complex (CPC), which plays multiple roles during mitosis and meiosis that are regulated in part by the PP2A phosphatase complex (Saurin, 2018). At the beginning of the M phase, the CPC is localized to chromosomes, where it controls chromatin-dependent spindle assembly, inhibition of nuclear assembly, and processes at the centromere and kinetochore, such as inner and outer kinetochore assembly, the spindle assembly checkpoint (SAC), and the correction of erroneously attached kinetochore-microtubules (Carmena *et al.*, 2012; Hindriksen *et al.*, 2017). The discrete localization of the CPC to chromosome arms, centromeres, and kinetochores is thought to be important for mediating different functions of the CPC (Campbell and Desai, 2013; Bonner *et al.*, 2019; Fischböck-Halwachs *et al.*, 2019; Hadders *et al.*, 2020; Broad *et al.*, 2020). However, the mechanisms by which the CPC is recruited to these different chromosome elements are not completely understood.

The CPC interacts with chromatin through its CEN module, which consists of Survivin, Borealin, and the N-terminus of INCENP (Jeyaprakash *et al.*, 2007). Borealin contributes directly to the interaction with chromatin by binding to DNA and to the acidic patch formed between histones H2A and H2B on the nucleosome core (Abad *et al.*, 2019). However, the Borealin–acidic patch interaction is not sufficient for the effective and specific recruitment of the CPC, which also requires the phosphorylation of histones by the mitotic

This article was published online ahead of print in MBoC in Press (http://www.molbiolcell.org/cgi/doi/10.1091/mbc.E20-05-0341) on July 22, 2020.

[†]These authors contributed equally to this work.

Competing financial interests: The authors declare no competing financial interests.

Author contributions: M.K.B., J.H., H.S., and A.E.K. designed the experiments; M.K.B., J.H., H.S., H.G., B.I.L., and A.E.K performed and/or analyzed experiments. M.K.B. and A.E.K. wrote the manuscript with input from all co-authors.

Present address: [‡]Tetrad Graduate Program, University of California, San Francisco, San Francisco, CA 94143; [§]Pediatric Oncology Branch, National Cancer Institute, NIH, Bethesda, MD 20892.

*Address correspondence to: Alexander Kelly (alexander.kelly@nih.gov).

Abbreviations used: CPC, chromosomal passenger complex; SAC, spindle assembly checkpoint.

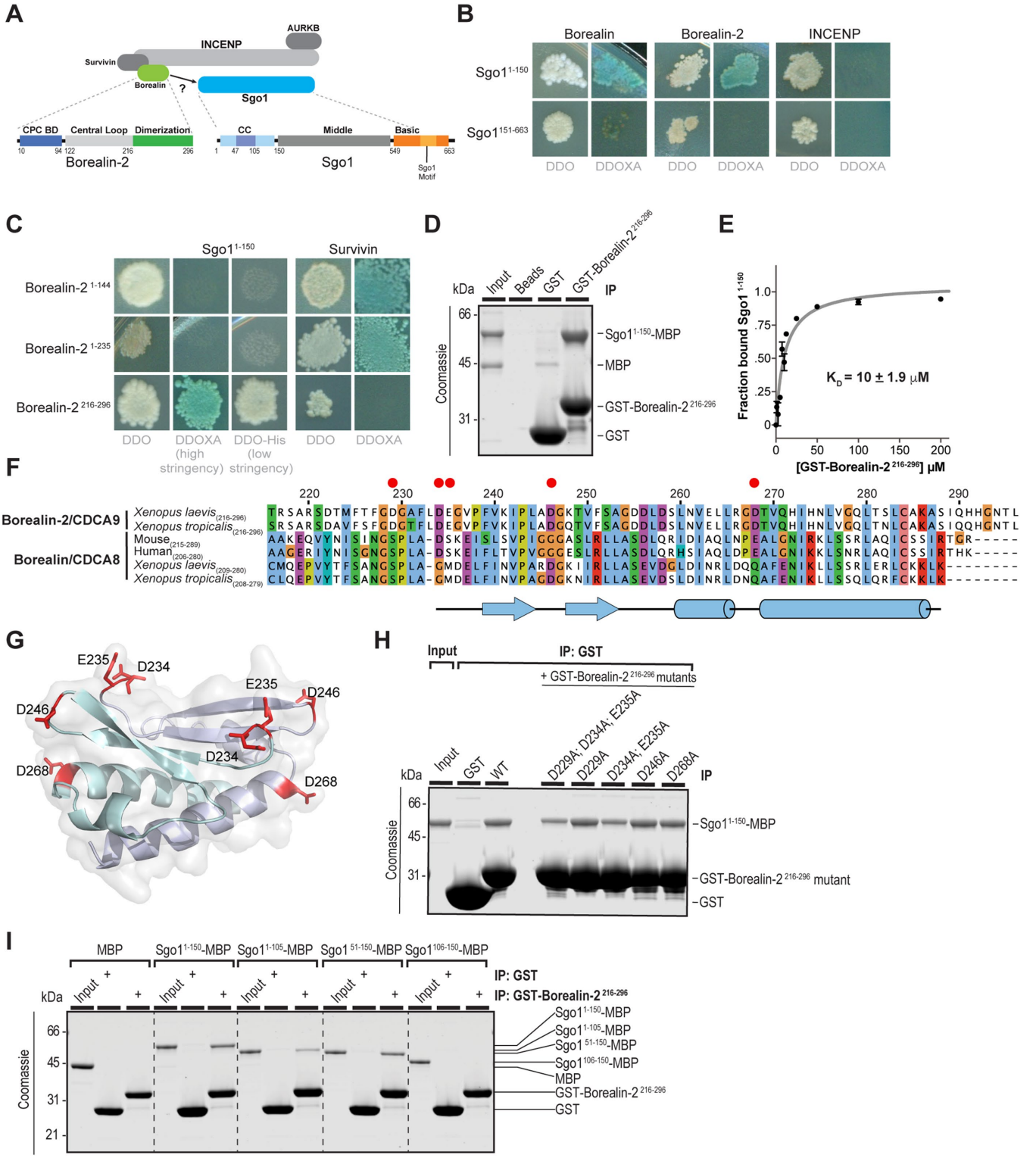

FIGURE 1: Direct binding of the Borealin C-terminal dimerization domain to Sgo1. (A) Schematic of the chromosomal passenger complex (CPC), which includes Aurora B kinase (AURKB), INCENP, Borealin-2, and Survivin. Aurora B kinase binds to the C-terminal INbox domain of INCENP, and Borealin-2 and Survivin bind to the N-terminal centromere targeting domain of INCENP. Borealin-2 contains three domains: an N-terminal coiled-coil domain through which it interacts with Survivin and INCENP, an unstructured central loop region that binds to nucleosomes, and a C-terminal dimerization domain. Sgo1 contains three domains: an N-terminal coiled-coil domain, a middle domain, and a C-terminal basic domain that includes the Sgo1 motif that interacts with H2AT120ph nucleosomes. (B) Yeast two-hybrid (Y2H) interactions of Sgo1 fragments with Borealin, Borealin-2, and INCENP. White colonies on the left are representative of diploid growth (DDO); blue colonies on the right represent interactions occurring on selective media (DDOXA). Borealin and Borealin-2 interact with Sgo1$^{1–150}$ but not Sgo1$^{151–663}$. INCENP shows no interaction with Sgo1. Images are

kinases Haspin and Bub1. Haspin phosphorylates histone H3 at threonine 3 (H3T3ph), which promotes direct interaction between the histone H3 N-terminal tail and the BIR domain of Survivin (Kelly *et al.*, 2010; Wang *et al.*, 2010; Yamagishi *et al.*, 2010). The H3T3ph mark directs accumulation of the CPC at the inner centromere and the chromosome arms (Kelly *et al.*, 2010; Broad *et al.*, 2020; Hadders *et al.*, 2020). How Bub1 kinase drives the interaction of the CPC with chromosomes is less clear. Bub1 kinase phosphorylates histone H2A at threonine 120 (H2AT120ph), which promotes the recruitment of the Shugoshin proteins (Sgo1 and Sgo2) to chromosome arms and to kinetochore-proximal centromeric chromatin (Rivera and Losada, 2009; Kawashima *et al.*, 2010; Tsukahara *et al.*, 2010; Yamagishi *et al.*, 2010; Liu *et al.*, 2013a; Broad *et al.*, 2020; Hadders *et al.*, 2020).

Sgo1 and/or Sgo2 are important for the proper localization and function of the CPC during meiosis and mitosis, but the mechanisms that underlie this pathway remain poorly characterized. Previous mutational analyses led to the suggestion that CDK1-dependent phosphorylation of a disordered region within Borealin promotes its direct interaction with the coiled coil domains of Sgo1/2 to mediate the Bub1-dependent recruitment of the CPC to chromosomes (Tsukahara *et al.*, 2010). However, a direct interaction between the Borealin disordered region and Sgo1/2 has not been demonstrated. In addition, several lines of evidence suggest that CDK1-dependent phosphorylation may affect other functions of Borealin and the CPC. First, the Borealin disordered region has been shown to mediate the interaction of the CPC with the nucleosome core (Abad *et al.*, 2019), suggesting an alternative basis for the observed defects in CPC recruitment caused by Borealin phosphorylation mutants. Second, a recent study demonstrated that CDK1-dependent phosphorylation of Borealin promotes the phase separation of the CPC CEN module but is not necessary for the incorporation of Sgo1 into CPC-mediated condensates, raising the possibility that CDK1 phosphorylation may not directly contribute to the CPC-Sgo1 interaction (Trivedi *et al.*, 2019b).

The coiled-coil domains of Sgo1/2 also interact with the PP2A phosphatase, which opposes Aurora B activity (Foley *et al.*, 2011; Foley and Kapoor, 2013; Vallardi *et al.*, 2019) and regulates Haspin recruitment through the protection of cohesin (Yamagishi *et al.*, 2010; Liu *et al.*, 2013a; Meppelink *et al.*, 2015; Hengeveld *et al.*, 2017; Liang *et al.*, 2020), indicating that Sgo1/2 may also contribute to CPC localization and activity through recruitment of PP2A. Thus, how and whether Sgo1/2 directly recruits the CPC to chromosomes and its importance to CPC function remain unclear (Hindriksen *et al.*, 2017).

Here, we show that the dimerization domain of Borealin binds directly to the coiled-coil domain of Sgo1. We find that Borealin and PP2A bind different residues in the Sgo1 coiled-coil domain and that Borealin and PP2A can bind simultaneously to the same region of Sgo1, which has important implications for the regulation of Aurora B–mediated error correction. The Borealin–Sgo1 interaction plays a critical role in the recruitment of the CPC to chromosomes, and is necessary for proper spindle assembly. Finally, we show that the Borealin–Sgo1 interaction is not required for SAC signaling at unattached kinetochores, demonstrating that the CPC–Sgo1 interaction plays discrete roles in regulating CPC and Aurora B functions.

RESULTS AND DISCUSSION

The Borealin dimerization domain interacts directly with the Sgo1 coiled coil

Bub1 kinase is important for the recruitment of the CPC to chromosomes in *Xenopus laevis* egg extracts (Boyarchuk *et al.*, 2007). Although both Sgo1 and Sgo2 recruitment require Bub1 activity, only Sgo1 contributes to CPC recruitment (Rivera *et al.*, 2012). We therefore focused on understanding the molecular basis of the CPC–Sgo1 interaction in *X. laevis* (Supplemental Figure S1A). We first investigated the interaction between Sgo1 and the *X. laevis* Borealin paralogs (Borealin/CDCA8/Dasra B and Borealin-2/CDCA9/Dasra A; Sampath *et al.*, 2004; Kelly *et al.*, 2007; Figure 1A). Yeast two-hybrid analysis showed that Sgo1$^{1\text{-}150}$ binds to both Borealin paralogs, but not to INCENP, under stringent selection (Figure 1B and Supplemental Figure S1B). Thus, the *X. laevis* Borealin paralogs interact with the N-terminus of Sgo1, in line with a previously reported interaction between human Sgo1 and Borealin (Tsukahara *et al.*, 2010). We could detect no additional interactions of Borealin-2 with other regions of Sgo1 and found that Borealin-2 can self-associate, as does human Borealin (Bourhis *et al.*, 2009; Figure 1B and Supplemental Figure S1C). This suggests that both Borealin paralogs interact with the Sgo1 N-terminus in a similar manner, and hereafter we will examine the interaction between Sgo1 and Borealin-2, the embryonic form of Borealin found in *Xenopus* egg extracts (Wühr *et al.*, 2014; Presler *et al.*, 2017), which henceforth will be referred to simply as Borealin.

representative of four separate experiments. Representative positive and negative Y2H controls used throughout are shown in Supplemental Figure S1B. (C) Y2H interactions of Borealin-2 fragments with Sgo1$^{1–150}$ and Survivin. Borealin-2$^{1–144}$ and Borealin-2$^{1–235}$ interact with Survivin but not Sgo1$^{1–150}$, even under low stringency, and Borealin-2$^{216–296}$ interacts with Sgo1$^{1–150}$. Images are representative of four separate experiments. See also Supplemental Figure S1, C and D. (D) Binding assay showing GST-Borealin-2$^{216–296}$ interaction with Sgo1$^{1–150}$ -His$_6$-MBP. Colloidal Coomassie staining of SDS–PAGE gel including input and beads is shown. The input represents 7% total Sgo1$^{1–150}$-His$_6$-MBP incubated with beads. (E) Equilibrium assay to measure affinity of GST-Borealin-2$^{216–296}$ for Sgo1$^{1–150}$-His$_6$-MBP. Increasing amounts of GST-Borealin-2$^{216–296}$-bound glutathione sepharose 4B beads were titrated into Sgo1$^{1–150}$-His$_6$-MBP at 2 μM. Beads were pelleted, and samples of the supernatant were separated by SDS–PAGE to determine the fraction bound (see *Materials and Methods* and Supplemental Figure S1E). Curve is best fit of data to one-site binding equation yielding equilibrium constant of 10 μM. (F) Protein sequence alignment of the dimerization domains from Borealin-2 and Borealin-1 from indicated species. Clustalx coloring was applied to indicate conservation. Numbering denotes amino acid positions from *X. laevis* Borealin-2. Red circles mark amino acids featured in Figure 1G and mutated in Figure 1H. (G) Homology model of the *X. laevis* Borealin-2 (CDCA9/Dasra A) dimerization domain based on PDB ID: 2KDD (Bourhis *et al.*, 2009), showing surface-exposed acidic residues. Each monomer is indicated by separate colors. (H) Binding assay showing how mutations in Borealin-2 dimerization domain affect GST-Borealin-2$^{216–296}$ interaction with Sgo1$^{1–150}$-His$_6$-MBP. Coomassie staining of SDS–PAGE gel including input and beads is shown. The input represents 10% of total Sgo1$^{1–150}$-His$_6$-MBP incubated with beads. (I) Binding assay showing GST-Borealin-2$^{216–296}$ interaction with Sgo1-His$_6$-MBP truncations. Colloidal Coomassie staining of SDS–PAGE gel including input and beads is shown. The input represents 10% Sgo1-His$_6$-MBP variants incubated with beads.

Borealin contains three conserved and functionally distinct regions (Figure 1A). The N-terminus is responsible for mediating the interactions with Survivin and INCENP as well as contributing to the affinity for nucleosomes (Jeyaprakash *et al.*, 2007; Abad *et al.*, 2019). A disordered central loop interacts with nucleosomes (Abad *et al.*, 2019), mediates the formation of biomolecular condensates (Trivedi *et al.*, 2019b), and also contains a putative Sgo1-binding site (Tsukahara *et al.*, 2010). Finally, the C-terminal domain forms a symmetric homodimer that mediates CPC dimerization (Bourhis *et al.*, 2009). Yeast two-hybrid analysis demonstrated that neither Borealin$^{1–144}$ nor Borealin$^{1–235}$ could interact with Sgo1$^{1–150}$, even using low-stringency selection, although they did both interact with Survivin (Figure 1C). The lack of an interaction between the Borealin$^{1–235}$ fragment and Sgo1 was surprising, because this contains the region previously suggested to mediate the CPC-Sgo1 interaction (Tsukahara *et al.*, 2010). Strikingly, we found that that the Borealin C-terminal dimerization domain (Borealin$^{216–296}$) interacts with Sgo1$^{1–150}$. This interaction is specific, because we detected no interaction of Borealin$^{216–296}$ with Survivin, INCENP, or other fragments of Sgo1 (Figure 1C and Supplemental Figure S1D).

The interaction between Sgo1$^{1–150}$ and the dimerization domain was confirmed using purified proteins. Pulldowns showed that Sgo1$^{1–150}$ interacts specifically with the Borelian dimerization domain, validating our yeast two-hybrid analyses (Figure 1D). Using a bead-based equilibrium binding assay (Lee *et al.*, 2000; Pollard, 2010), we found that Sgo1$^{1–150}$ interacts with the Borealin dimerization domain with moderate affinity (K_d = 10.0 ± 1.6 μM; Figure 1E and Supplemental Figure S1E) and that the interaction data were best fitted by a one-site binding curve (unpublished data). Because *X. laevis* Sgo1$^{1–150}$ can self-associate (Xu *et al.*, 2009; Supplemental Figure S1F), these results suggest that a dimer of Sgo1 binds a dimer of Borealin.

We next sought to identify specific residues that contribute to the interaction between Borealin and Sgo1. The predicted isoelectric point of Sgo1$^{1–150}$ is quite basic (pI ~ 11), suggesting that Sgo1 may interact with acidic residues within the conserved Borealin dimerization domain. Sequence alignment and homology modelling indicated that Borealin residues 234 to 287 are ordered, whereas residues 216 to 233 are predicted to be disordered (Figure 1, F and G; Bourhis *et al.*, 2009). Therefore, we generated alanine mutants of surface-exposed acidic residues within Borealin$^{216–296}$ that are predicted not to perturb the structure of the dimerization domain (Figure 1G) and tested their contribution to the interaction with Sgo1$^{1–150}$ by in vitro pulldown. We found that mutation of residues Asp^{234} and Glu^{235} decreased Sgo1 binding, whereas mutation of other surface-exposed residues had no effect (Figure 1H). Although the Borealin dimerization domain does not contain any predicted CDK1 phosphorylation sites previously suggested to be required for the Borealin–Sgo1 interaction (Tsukahara *et al.*, 2010), Asp^{229} aligns with the CDK1-phosphorylated Ser^{219} of human Borealin (Figure 1F; Date *et al.*, 2012), suggesting that a negative charge at this position could be important. However, mutation of Asp^{229}, either alone (D229A) or in combination (D229A, D234A, E235A), did not affect the Sgo1–Borealin interaction (Figure 1H). These data suggest that residues Asp^{234} and Glu^{235} constitute part of a binding site for the N-terminus of Sgo1 on the surface of the Borealin dimerization domain (Figure 1G).

To further resolve the regions of Sgo1$^{1–150}$ responsible for interaction with the Borealin dimerization domain, we performed pulldown analysis using a series of truncations of Sgo1$^{1–150}$ (Figure 1A and Supplemental Figure S1G). Pulldown assays with purified proteins showed that deleting the N-terminal 50 residues of Sgo1 does not affect its interaction with Borealin, but that removal of residues C-terminal to the predicted coiled coil of Sgo1 (106–150) weaken the interaction (Figure 1I). This suggests either that the coiled-coil region interacts with Borealin and the C-terminal truncation of residues 106–150 destabilizes the coiled coil (as observed for human Sgo1; Xu *et al.*, 2009) or that the poorly conserved residues C-terminal to the coiled coil are also important for binding (Supplemental Figure S1G). However, the C-terminal fragment could not detectably bind Borealin on its own under our assay conditions. Thus, our data indicate that the coiled-coil domain of Sgo1 interacts with the dimerization domain of Borealin (Tsukahara *et al.*, 2010).

Borealin can interact with Sgo1 when it is bound to the PP2A complex

The PP2A phosphatase also binds to the coiled coil region of Sgo1 to carry out its functions (Xu *et al.*, 2009; Meppelink *et al.*, 2015; Saurin, 2018; Eshleman and Morgan, 2014; Verzijlbergen *et al.*, 2014; Liu *et al.*, 2013b), and almost all the Sgo1 in *Xenopus* egg extracts is found in complex with PP2A (Rivera *et al.*, 2012). Thus, we next sought to test whether Borealin can interact with PP2A-bound Sgo1. To begin to address this, we generated a Sgo1$^{1–150}$ construct that harbored three point mutations predicted to disrupt the Sgo1—PP2A interaction but not the dimerization of its coiled coil (Y57A, N60A, T62A; "Sgo1$^{1–150}$-3A"; Figure 2A and Supplemental Figure S1H; Xu *et al.*, 2009). Yeast two-hybrid analysis showed that Sgo1$^{1–150}$-3A could still interact with Borealin$^{216–296}$ and retained the ability to self-associate (Figure 2, B and C). To confirm that the Sgo1-3A mutant perturbed PP2A complex but not Borealin binding, we expressed Sgo1$^{1–150}$-GFP and Sgo1$^{1–150}$-3A-GFP from mRNA in *Xenopus* egg extract and performed immunoprecipitation of each protein. Sgo1$^{1–150}$-GFP was able to pull down PP2A (as indicated by the presence of PP2A-C, the catalytic subunit of PP2A), whereas Sgo1$^{1–150}$-3A-GFP was not (Figure 2D). In agreement with our yeast two-hybrid assays, both Sgo1$^{1–150}$-GFP and Sgo1$^{1–150}$-3A-GFP were able to pull down both INCENP and Borealin from egg extracts (Figure 2D), indicating that the three amino acids in Sgo1 that are important for PP2A binding are not essential for CPC binding. This suggests that Borealin and PP2A bind to distinct interfaces on the Sgo1 dimer, raising the possibility that Sgo1 can bind Borealin and PP2A simultaneously. To test this suggestion, we asked whether Sgo1 can form a co-complex with both PP2A and Borealin by immunoprecipitation of GST-Borealin$^{216–296}$ in the presence of substoichiometric amounts of Sgo1$^{51–150}$-MBP and PP2A (Figure 2E). A PP2A complex containing the catalytic subunit PP2A-C, the scaffolding subunit PP2A-A, and the PP2A-B56γ regulatory subunit that specifically binds Sgo1 in *Xenopus* egg extracts (Rivera *et al.*, 2012) was produced by in vitro translation. Strikingly, GST-Borealin$^{216–296}$ specifically pulled down the PP2A-B56γ complex, but only in the presence of Sgo1$^{51–150}$-MBP (Figure 2F). This demonstrates that Sgo1-Borealin and Sgo1-PP2A interaction are not mutually exclusive, and that the N-terminus of Sgo1 can bind both Borealin and PP2A simultaneously.

The Borealin–Sgo1 interaction regulates CPC recruitment to chromosomes to promote proper spindle assembly

CPC localization to chromosome arms and centromeric regions depends on multiple mechanisms that promote its interaction with nucleosomes, including direct interactions with the nucleosome core (Abad *et al.*, 2019), with the T3ph-modified histone H3 tail (Kelly *et al.*, 2010; Wang *et al.*, 2010; Yamagishi *et al.*, 2010), and Sgo1 (Tsukahara *et al.*, 2010). However, the multiple roles that Sgo1 plays in mitosis (Hindriksen *et al.*, 2017) have confounded assessment of

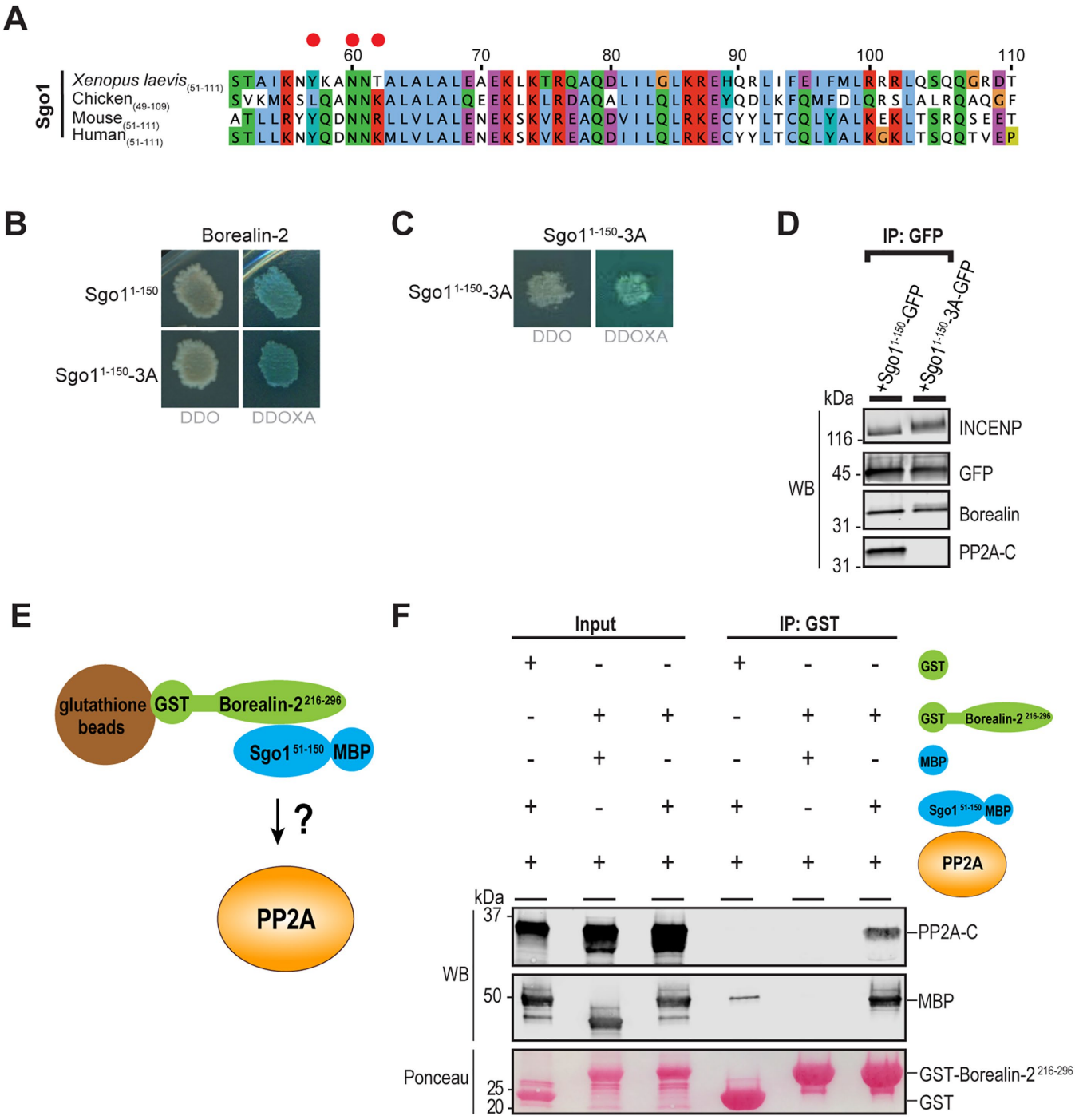

FIGURE 2: Borealin and PP2A can bind simultaneously to the Sgo1 coiled coil. (A) Sequence alignment of the N-terminal coiled-coil region of Sgo1 in indicated species. Clustalx coloring was applied to indicate conservation in sequence alignment. Numbering denotes amino acid positions from *X. laevis* Sgo1. Red circles indicate amino acids mutated in Sgo1$^{1–150}$-3A, a mutant that cannot bind to PP2A. (B) Y2H interactions of Borealin-2 with Sgo1$^{1–150}$ and Sgo1$^{1–150}$-3A (Y57A, N60A, T62A). Borealin-2 interacts with both Sgo1$^{1–150}$ and Sgo1$^{1–150}$-3A. Images are representative of four separate experiments. See also Supplemental Figure S1F. (C) Y2H interactions of Sgo1$^{1–150}$-3A with Sgo1$^{1–150}$-3A. Sgo1$^{1–150}$-3A interacts with itself. Images are representative of four separate experiments. (D) Western blot for proteins that copurify with Sgo1$^{1–150}$-GFP or Sgo1$^{1–150}$-3A-GFP (Y57A, N60A, T62A) expressed from mRNA in *Xenopus* egg extracts. IP, immunoprecipitated. (E) Schematic of co-binding experiment performed to investigate whether Sgo1$^{51–150}$-His$_6$-MBP can bind to GST-Borealin-2$^{216–296}$ and PP2A complex simultaneously. (F) Western blot for proteins that co-purify with GST or GST-Borealin-2$^{216–296}$ in co-binding experiment. Ponceau indicates loading of GST or GST-Borealin-2$^{216–296}$.

the relative importance of Sgo1 in CPC localization. To test this, we depleted endogenous CPC from *Xenopus* egg extracts, replaced it with CPC containing GFP-tagged versions of Borealin dimerization domain truncations, and determined the levels of INCENP and Borealin-GFP on chromosomes by immunofluorescence (Figure 3A). Consistent with previous findings (Kelly *et al.*, 2007; Haase *et al.*,

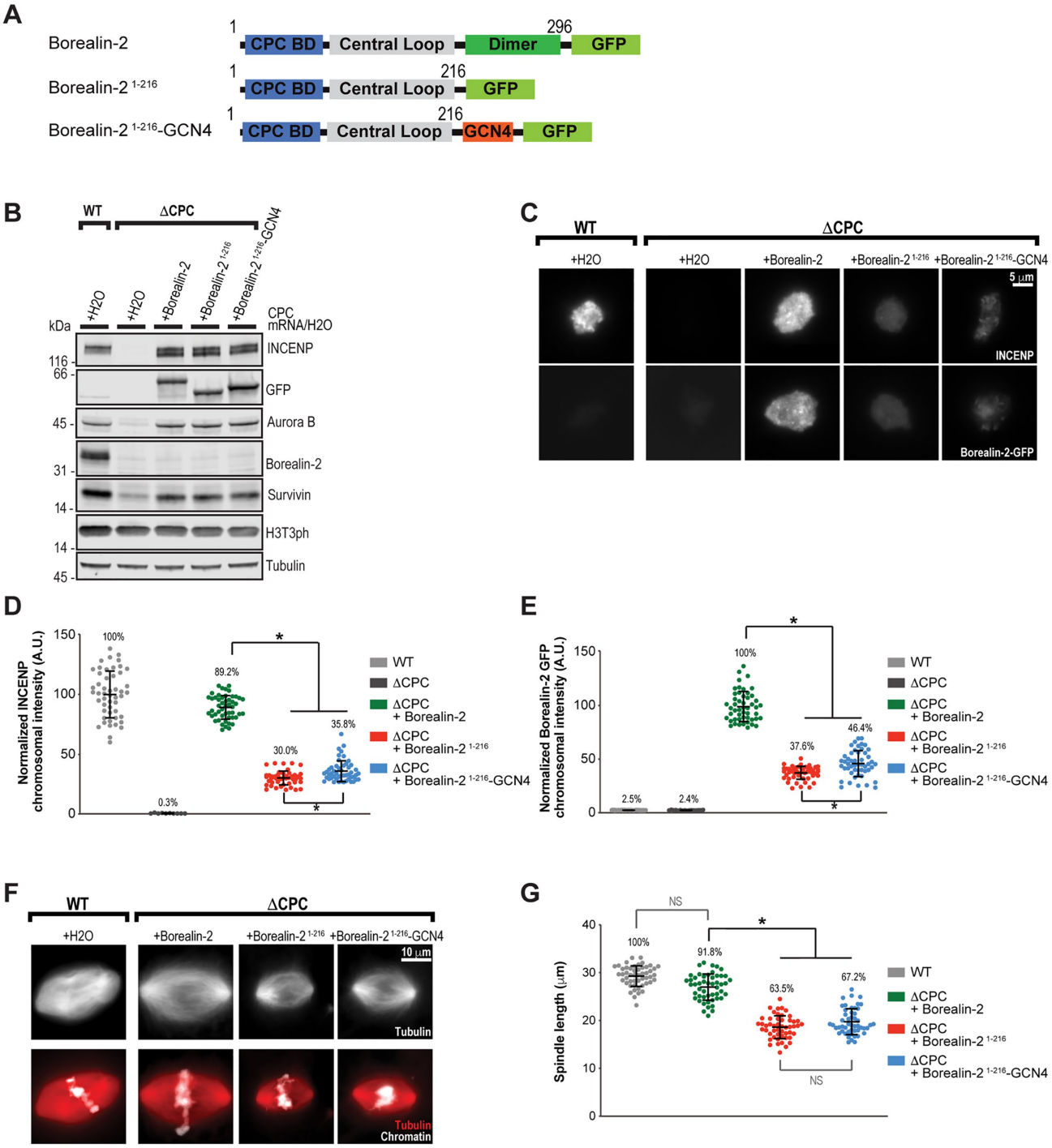

FIGURE 3: The Borealin–Sgo1 interaction controls CPC loading onto chromosome arms to promote spindle assembly. (A) Schematic of Borealin-2 constructs used to express mRNAs in *Xenopus* egg extract, along with full-length versions of other CPC components, Aurora B, INCENP, and Survivin. All four constructs were expressed to reconstitute the CPC in ΔCPC extracts. (B) Western blot for INCENP, GFP, Aurora B, Borealin-2, Survivin, histone H3 phosphorylation (H3T3ph), and tubulin for samples from *Xenopus* wild-type and or CPC-depleted (ΔCPC) metaphase extracts with indicated CPC variants expressed from mRNA. (C) Representative immunofluorescence (IF) images of replicated chromosomes in wild-type and ΔCPC metaphase extracts with indicated CPC variants (Western blot for samples shown in B). Chromosomes were stained for INCENP and Borealin-2-GFP. See also Supplemental Figure S2A. (D) Quantification of fluorescence intensity of INCENP was normalized to wild-type condition. $n = 50$ chromatin structures per condition. Error bars represent SD unless otherwise noted, and asterisks indicate a statistically significant difference (*, $p < 0.001$). A.U., arbitrary units. (E) Quantification of fluorescence intensity of Borealin-2 GFP was normalized to Borealin-2-GFP condition. $n = 50$ chromatin structures per condition. (F) Top: Representative IF images of spindles formed in wild-type and ΔCPC extracts with indicated CPC conditions. Rhodamine-labeled tubulin was added to visualize microtubules (white). Bottom: Chromatin was stained with Hoechst (white), and rhodamine-labeled tubulin was added to visualize microtubules (red). (G) Quantification of bipolar spindle length. $n = 50$ spindles per condition.

2017), CPC depletion led to complete loss of INCENP at chromosomes (Figure 3, B–E, and Supplemental Figure S2A). Addition of CPC including wild-type Borealin rescued the chromosomal localization of INCENP (89.2% of mock-depleted) and promoted robust localization of Borealin-GFP to chromosomes. In contrast, the levels of INCENP and Borealin-GFP on chromosomes in extracts complemented with Borealin$^{1–216}$-GFP, which removes the dimerization domain, were severely diminished (30.0% of mock-depleted and 37.6% of Borealin-GFP, respectively; Figure 3, B–E, and Supplemental Figure S2A). In support of this, mutation of the Borealin dimerization domain has previously been reported to decrease the abundance of the CPC at centromeres in human cells (Liu *et al.*, 2014). This mutation (V231E) is likely to disrupt the tertiary structure of Borealin, as Val^{231} is buried within the hydrophobic core of each monomer of the dimerization domain (Figure 1F; Bourhis *et al.*, 2009), and have a similar effect in disrupting Sgo1 binding as our truncation mutant. Thus, the Borealin dimerization domain plays a conserved role in the recruitment of the CPC to chromosomes.

Borealin dimerization has been shown to increase the affinity of the CPC for histone H3T3ph-modified nucleosomes indirectly through avidity effects (Abad *et al.*, 2019), and thus Borealin may contribute to CPC localization through dimerization of the CPC (Bekier *et al.*, 2015) and through mediating the interaction with Sgo1. To test this, we replaced the Borealin dimerization domain with the leucine-zipper motif from GCN4 (O'Shea *et al.*, 1991) to artificially drive Borealin dimerization in the absence of an interaction with Sgo1. In vitro immunoprecipitations from rabbit reticulocyte lysates confirmed that the GCN4 motif specifically promotes the self-association of Borealin lacking the dimerization domain (Supplemental Figure S2B). We found that extracts containing artificially dimerized Borealin$^{1–216}$-GCN4 had reduced chromosomal levels of INCENP and Borealin-GFP (35.8% and 46.4%, respectively) indicating that dimerization alone is insufficient to promote full CPC localization (Figure 3, B–E, and Supplemental Figure S2A). However, we did observe a statistically significant increase (~1.2-fold) in CPC levels when compared with Borealin$^{1–216}$, likely attributable to an increased affinity for H3T3ph nucleosomes. Interestingly, the CPC localization defects caused by disruption of the Borealin–Shugoshin interaction are more severe than those caused by elimination of H3T3ph (Kelly *et al.*, 2010; e.g., Borealin recruitment; 37.6% vs. ~60% of control). Thus, we conclude that the interaction of the Borealin dimerization domain with Sgo1 plays a major role in CPC recruitment to chromosomes in *Xenopus* egg extracts.

CPC binding to the chromosome arms drives local Aurora B activation in *Xenopus* egg extracts, which in turn promotes spindle assembly by suppressing microtubule-depolymerizing activities around chromosomes (Sampath *et al.*, 2004; Kelly *et al.*, 2007; Zhang *et al.*, 2007). Inhibition of the interaction between the CPC and histone H3T3ph leads to only partial disruption of CPC chromosomal levels and spindle length (Kelly *et al.*, 2010; Rivera *et al.*, 2012), while removal of the CPC from chromosomes completely blocks spindle assembly (Kelly *et al.*, 2007). We therefore hypothesized that the Borealin–Sgo1 interaction may also be important for proper spindle assembly. To test this, we measured spindle length in egg extracts where the endogenous CPC was replaced by CPC containing the Borealin constructs described above. CPC containing wild-type Borealin-GFP resulted in normal-length spindles, whereas CPC containing either Borealin$^{1–216}$-GFP or Borealin$^{1–216}$-GCN4-GFP resulted in 36.5% and 32.8% reduction in spindle length (Figure 3, F and G). Thus, the interaction between the Borealin dimerization domain and Sgo1 is important for the recruitment of the CPC to chromosomes for proper spindle assembly.

Our findings are consistent with and extend previous results demonstrating a role for Sgo1 in the recruitment of the CPC to chromosomes (Rivera *et al.*, 2012; Meppelink *et al.*, 2015) and the importance of CPC levels on chromosomes in regulating spindle length (Kelly *et al.*, 2007; Tseng *et al.*, 2010). However, in contrast to our results here, Rivera *et al.* (2012) reported that the depletion of Sgo1 from egg extracts had no effect on spindle length. A likely explanation for this difference in phenotypes is that depletion of Sgo1 would also drastically reduce phosphatase levels on chromosomes, because in egg extracts Sgo1 is almost entirely in complex with the PP2A–B56γ complex (Rivera *et al.*, 2012), and because Sgo1 has been shown to regulate the chromosomal distribution of other PP2A complexes in human cells (e.g., B56α and B56ε; Vallardi *et al.*, 2019). This reduction in chromosomal phosphatase levels in turn could counteract the partial loss of the CPC from chromosomes, through increased Aurora B activity and consequent stimulation of downstream microtubule nucleation and assembly pathways. Indeed, Aurora B autophosphorylation levels are maintained in Sgo1-depleted egg extracts and human cells despite reductions in the amount of Aurora B on chromosomes (Rivera *et al.*, 2012; Meppelink *et al.*, 2015). Furthermore, total inhibition of PP2A by okadaic acid in egg extracts leads to increased phosphorylation of INCENP residues necessary for full Aurora B activity (Kelly *et al.*, 2007), increased Aurora B-dependent phosphorylation of Op18 that promotes spindle assembly (Gadea and Ruderman, 2006; Kelly *et al.*, 2007; Andersen *et al.*, 1997), and increased phosphorylation of other CPC subunits (Supplemental Figure S2C). In contrast, our experiments specifically inhibited the Sgo1–Borealin interaction. Because Sgo1 recruitment to chromatin has been shown to be independent of the CPC (Boyarchuk *et al.*, 2007; Broad *et al.*, 2020; Hadders *et al.*, 2020), this should still allow Sgo1 and PP2A recruitment to chromosome arms, resulting in reduced Aurora B–mediated microtubule assembly around chromosomes (Figure 3, F and G).

Sgo2 has been reported play a role in spindle assembly, but not CPC localization, in *Xenopus* egg extracts (Rivera *et al.*, 2012). Sgo2 recruits the microtubule depolymerase MCAK to centromeres, but not chromosome arms, to regulate kinetochore-microtubule attachment (Zhang *et al.*, 2007; Tanno *et al.*, 2010), and Sgo2 depletion from egg extracts causes monopolar spindles and chromosome misalignment (Rivera *et al.*, 2012). We did not observe any defects in chromosome alignment or spindle polarity in our Borealin mutants (Figure 3, F and G), which suggests that the Borealin dimerization domain is not necessary for Sgo2-mediated spindle assembly. Altogether, our data suggest that Sgo1 and the phosphorylated histone H3 tail (H3T3ph) represent the main receptors for the CPC on chromosome arms and coordinate to promote Aurora B-mediated spindle assembly in *Xenopus* egg extracts.

Borealin dimerization is sufficient for Aurora B-mediated SAC signaling at kinetochores

Recent work has demonstrated that the CPC is independently enriched in multiple discrete pools at centromeres and kinetochores in early mitosis (Yue *et al.*, 2008; Caldas *et al.*, 2013; Campbell and Desai, 2013; Bekier *et al.*, 2015; Haase *et al.*, 2017; Hengeveld *et al.*, 2017; Bonner *et al.*, 2019; Fischböck-Halwachs *et al.*, 2019; García-Rodríguez *et al.*, 2019; Broad *et al.*, 2020; Hadders *et al.*, 2020; Liang *et al.*, 2020). Interestingly, in human cells, the mitotic checkpoint can be supported even when both Haspin kinase and Bub1 kinase are inhibited, suggesting that the recruitment of the CPC by histone H3T3ph and Sgo1/2 is not necessary for the SAC (Broad *et al.*, 2020; Hadders *et al.*, 2020). In agreement with those studies, we previously showed in *Xenopus* egg extracts that artificial

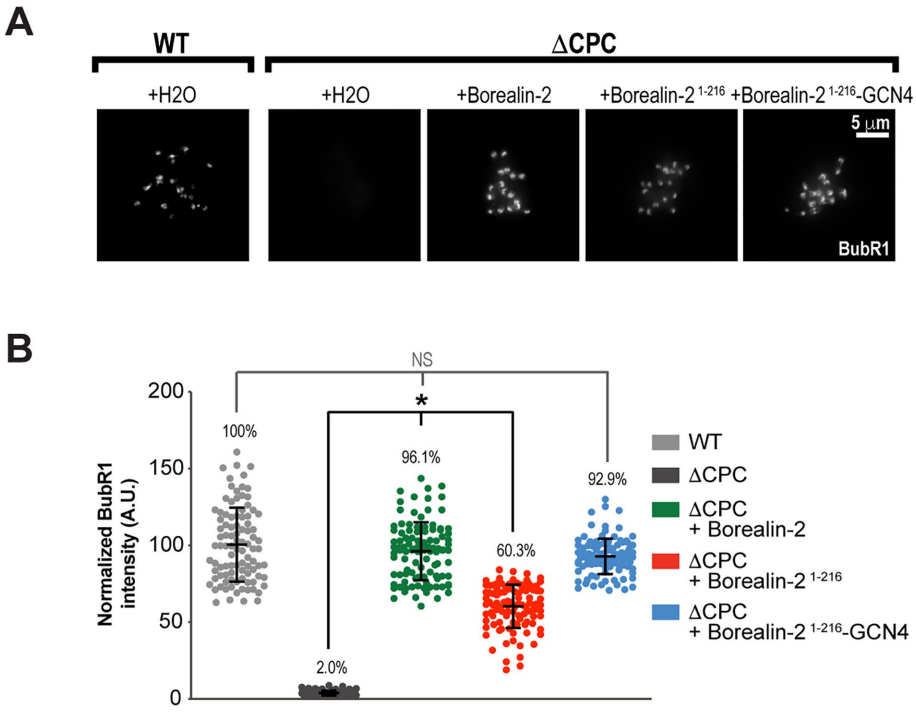

FIGURE 4: Artificial dimerization of Borealin is sufficient for CPC-mediated BubR1 enrichment at kinetochores. (A) Representative IF images of replicated chromosomes in wild-type and ΔCPC metaphase extracts with indicated CPC variants (Western blot for samples shown in Figure 3B). Kinetochores were stained for BubR1. (B) Quantification of fluorescence intensity of BubR1 was normalized to wild-type condition. $n = 100$ kinetochores per condition.

clustering of noncentromeric CPC lacking Borealin and Survivin is sufficient to promote full enrichment of the checkpoint protein BubR1 at unattached kinetochores (Haase *et al.*, 2017). To examine the spindle assembly checkpoint (SAC) response in the absence of the dimerization domain of Borealin, we measured BubR1 enrichment at unattached kinetochores. To our surprise, BubR1 levels decreased significantly when the dimerization domain of Borealin was absent (Figure 4, A and B), and artificial dimerization of Borealin by the GCN4 leucine zipper rescued BubR1 enrichment (Figure 4, A and B). These findings suggest that the interaction of Sgo1 with the Borealin dimerization domain is dispensable for BubR1 enrichment, but that dimerization of the CPC is necessary to promote a checkpoint response. One possible explanation is that dimerization is required for Aurora B auto-activation to reach a critical threshold that promotes SAC signaling (Sessa *et al.*, 2005; Kelly *et al.*, 2007; Zaytsev *et al.*, 2016; Musacchio and Desai, 2017). Alternatively, CPC dimerization may strengthen the interactions of the CPC with other recruitment sites that properly position Aurora B kinase for SAC-dependent substrate phosphorylation. In support of the latter suggestion, we previously reported that BubR1 enrichment is impaired when the CPC is unable to associate with the inner kinetochore through the central region of INCENP in egg extracts. This defect occurs even when Aurora B activity is high and the CPC retains its ability to dimerize and interact with Sgo1 through Borealin (Bonner *et al.*, 2019). Thus, our data suggest that Borealin dimerization may contribute to the enrichment of the CPC at kinetochores to promote SAC signaling, independently of its role in Sgo1-binding.

This study expands our knowledge of how the CPC is recruited to chromosomes through the discovery of a specific interaction between the C-terminal Borealin dimerization domain and the N-terminal coiled coil of Sgo1. Instead of a single high-affinity receptor, the CPC utilizes multiple moderate-affinity interactions to facilitate its recruitment to chromatin (Figure 5). This arrangement likely allows the discrete spatial and temporal regulation of Aurora B localization and activity in the early M phase that is required for its functions (Yue *et al.*, 2008; Caldas *et al.*, 2013; Campbell and Desai, 2013; Hengeveld *et al.*, 2017; Haase *et al.*, 2017; Bonner *et al.*, 2019; Fischböck-Halwachs *et al.*, 2019; García-Rodríguez *et al.*, 2019; Broad *et al.*, 2020; Hadders *et al.*, 2020). However, it remains unclear how different permutations of these binding modes are employed. Our discovery that the Sgo1-binding site on Borealin does not overlap with the regions of Borealin that mediate its interactions with nucleosomes and the CPC strongly suggests that all of the binding modes of the CPC can be utilized at the same time to interact with a single nucleosome (Figure 5). However, further studies will be required to understand if this can occur in vivo, and how processes such as transcription regulate CPC-Sgo1 and CPC-nucleosome interactions (Liu *et al.*, 2015; Blower, 2016). While we show that CDK1-dependent phosphorylation of Borealin is not necessary for the Borealin–Sgo1 interaction (Figure 1, D and H; Tsukahara *et al.*, 2010), it likely contributes to the overall strength of the CPC interaction with chromatin by lowering the concentration threshold for phase separation (Trivedi *et al.*, 2019b).

It is still unclear how Aurora B senses and responds to errors in kinetochore-microtubule attachment. The centromeric localization of the CPC and Aurora B is required for proper error correction, although it is not necessary for checkpoint signaling (Figure 4, A and B; Haase *et al.*, 2017; Broad *et al.*, 2020; Hadders *et al.*, 2020). Sgo1 is thought to play an important role in this process by recruiting the CPC and the phosphatase PP2A, which opposes Aurora B–mediated destabilization of attachments and thus allows the formation of new attachments after correction (Foley *et al.*, 2011; Meppelink *et al.*, 2015; Saurin, 2018). Our data indicate that Sgo1 can bring the PP2A complex into close proximity with the CPC. In turn, Sgo1-mediated colocalization of PP2A and the CPC might facilitate the dephosphorylation of CPC subunits to alter their activity and function (Elowe *et al.*, 2007; Kelly *et al.*, 2007; Wang *et al.*, 2011; Fink *et al.*, 2017; Wheelock *et al.*, 2017; Trivedi *et al.*, 2019a, 2019b). Consistent with this, we find that both INCENP and Borealin migrate more slowly when bound to the Sgo1-3A mutant in egg extracts. Because Sgo1-3A is defective in PP2A binding, this suggests that PP2A actively dephosphorylates the CPC when it is bound to Sgo1 (Figure 2D and Supplemental Figure S2C). Our elucidation of the Sgo1–CPC interaction and the potential for integration of PP2A activity is an important step toward a complete mechanistic understanding of how Aurora B and the CPC promote the biorientation of sister chromatids.

MATERIALS AND METHODS

Cloning

X. laevis Borealin, Borealin-2, Survivin, INCENP, Aurora B, Sgo1, PP2A-A (ppp2r1a-a), PP2A-B56γ (ppp2r5c), and PP2A-C (ppp2ca) were cloned into vectors pGBKT7, pGADT7, pCSII, pGEX-6P1, or

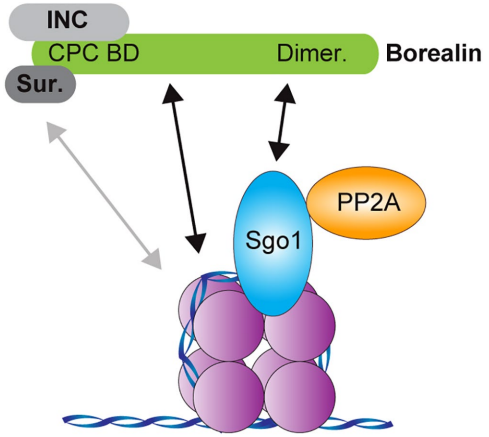

FIGURE 5: The CPC is recruited to chromatin through multiple mechanisms. Model for the multivalent recruitment of the CPC to chromatin. Survivin interacts with the histone H3T3ph tail (Kelly *et al.*, 2010; Du *et al.*, 2012; Niedzialkowska *et al.*, 2012; Jeyaprakash *et al.*, 2011), the Borealin N-terminus and its central loop interact with nucleosomes (Abad *et al.*, 2019), and the Borealin C-terminal dimerization domain interacts with Sgo1, which in turn interacts with histone H2AT120ph C-termini (Liu *et al.*, 2015b; Kawashima *et al.*, 2010) to recruit the CPC (the CEN module of the CPC is shown here: the N-terminus of INCENP, Survivin, and Borealin) to chromatin. It is currently unclear whether the H3T3ph and H2AT120ph marks are present on the same nucleosome. The N-terminal coiled-coil region of Sgo1 can interact with Borealin-2 and PP2A simultaneously, suggesting that both the CPC and PP2A may be recruited to the same nucleosome.

pET28 by Gibson assembly (NEB). Sequences for PP2A (A-C) and Sgo1 were obtained from a *X. laevis* cDNA library (Horizon). Point mutants in Sgo1 and in Borealin-2 were generated using the Q5 Site-Directed Mutagenesis kit (NEB).

Protein purification

MBP, Sgo1$^{1\text{-}150}$-His$_6$-MBP, and other truncations of Sgo1 (Sgo1$^{1\text{-}105}$-His$_6$-MBP, Sgo1$^{51\text{-}150}$-His$_6$-MBP, Sgo1$^{106\text{-}150}$-His$_6$-MBP) were expressed in LOBSTR BL21(DE3) Rosetta-2 cells (Andersen *et al.*, 2013). Cells were induced for 21 h with 0.1 mM IPTG at 18°C. The tagged proteins were bound to Ni-NTA agarose (Qiagen), washed with wash buffer (20 mM HEPES, pH 7.9, 50 mM imidazole, 300 mM NaCl, 5 mM β-mercaptoethanol), and eluted with elution buffer (20 mM HEPES, pH 7.9, 300 mM imidazole, 300 mM NaCl, 5 mM β-mercaptoethanol). Eluted proteins were dialyzed into 20 mM HEPES, pH 7.9, 150 mM NaCl, 1 mM TCEP. Borealin-2 or Borealin-2 mutants were expressed in BL21(DE3) Rosetta-2 cells (EMD Millipore). Cells were induced with 0.3 mM IPTG for 20 h at 18°C. The tagged proteins were bound to Glutathione Sepharose 4B resin (GE) and the beads were washed extensively with 20 mM HEPES, pH 7.9, 500 mM NaCl, 1 mM TCEP and exchanged into 20 mM HEPES, pH 7.9, 150 mM NaCl, 1 mM TCEP.

Yeast Two Hybrid

Y2H experiments were performed using the Matchmaker Gold system (630489, Clontech Laboratories) and designed using the provided protocols. In brief, potential interaction partners were cloned into both the Y2H bait (pGBKT7) and prey (pGADT7) plasmids as described above. Bait plasmids were then transformed into Y2H-Gold (MATa) and prey plasmids were transformed into Y187 (Matα). Bait strains were then mated to prey strains in 96-well plates. An overnight culture of an individual bait strain (100 µl) was mixed with an individual prey strain (100 µl) in a single well and incubated for 24 h at 32°C while being shaken at 150 RPM. A sample of 2–3 µl of each mating reaction was transferred to double dropout (DDO; SD-Leu-Trp) plates using a 48-pin multiblot replicator (VP 407AH, V&P Scientific) to select for diploids containing both bait and prey plasmids. After 3–5 d of growth, diploids were then replica-plated to DDOXA (SD-Leu-Trp +X-α-Gal [630463, Clontech Laboratories] + 200 ng/mL Aureobasidin A [630499, Clontech Laboratories]) plates and grown for 5 d at 32°C. Colonies were scored for growth and blue color on a scale ranging from 0 to 3 (no growth/color to robust growth/color, respectively). All possible interactions were tested four times in independent experiments. None of the interaction partners tested activated the Y2H reporters on their own in auto-activation assays performed by mating partners to "empty" prey or bait strains (unpublished data).

Xenopus egg extracts

Xenopus laevis egg extract was prepared, RNase-treated, and immunodepleted as previously described (Kelly *et al.*, 2007). To express the CPC in immunodepleted extract, we pooled CPC mRNAs (consisting of INCENP, Aurora B, Borealin-2 [CDCA9/Dasra A], and Survivin, unless otherwise indicated) and added them to extracts at the onset of interphase (Haase *et al.*, 2017). To assess spindle assembly and CPC or BubR1 recruitment, sperm chromatin was replicated in extracts during interphase, and spindles were assembled by addition of two volumes of CSF extract (Haase *et al.*, 2017). When the extract was driven into metaphase, nocodazole or okadaic acid was added as needed to a final concentration of 33 µM or 1 µM, respectively. A 1:200 dilution of a rhodamine-X-labeled bovine brain tubulin stock solution (10 mg/ml; Cytoskeleton) was added to observe the progress of spindle assembly. Metaphase spindle assembly was assayed by fixing 1 µl samples with Hoechst (10 µg/ml; Hoechst 33258, Invitrogen) and imaging tubulin and DNA. Samples for Western blot and immunofluorescence were taken once metaphase was successfully achieved.

Protein Binding Assays

GST-Borealin-2$^{216–296}$ in vitro binding assays. Binding assays were performed to determine whether Borealin-2$^{216–296}$ or Borealin-2$^{216–296}$ variants interact with Sgo1 truncations or variants. Sgo1 variants were incubated with GST or a GST-Borealin-2 variant bound to glutathione sepharose 4B resin for 1 h at 4°C with end-over-end rotation. Beads were washed three times with wash buffer (20 mM HEPES, pH 7.9, 150 mM NaCl, 1 mM TCEP) and eluted with 2X sample buffer.

Co-binding assay for Borealin-2, Sgo1, and PP2A. A co-binding assay was performed to determine whether Sgo1$^{51–150}$-His-MBP could cobind to both Borealin-2$^{216–296}$ and the PP2A-B56 complex. The PP2A complex was expressed via the in vitro transcription and translation (T_NT) system (Promega). Reticulocyte lysates (25 µl) containing expressed PP2A-56γ complex were incubated with 15 µM Sgo1$^{51–150}$-His$_6$-MBP or His$_6$-MBP and GST or GST-Borealin-2$^{216–296}$ bound to Glutathione Sepharose 4B beads (effective concentration 50 µM) with end-over-end rotation for 1 h at 4°C. Beads were then collected, washed five times with ice-cold wash buffer (20 mM HEPES, pH 7.9, 150 mM NaCl, 1 mM TCEP, 0.1% Triton-X), and eluted with 2X sample buffer.

Co-immunoprecipitations

Immunoprecipitations were performed to assess which proteins in *Xenopus* egg extract bind to Sgo1-GFP or variants. GFP or Sgo1-GFP variants were expressed from mRNA in *Xenopus* egg extract

without chromatin for 1 h at 20°C. GFP-Trap Magnetic Agarose beads (Chromotek) were added to extract and incubated with end-over-end rotation for 1 h at 4°C. Beads were then captured by magnetization, washed four times with wash buffer (10 mM HEPES, pH 7.7, 200 mM NaCl, 1 mM $MgCl_2$, 50 mM sucrose, 5 mM EGTA, 0.5 mM TCEP, 0.01% NP-40, 1X Leupeptin/Pepstatin/Chymostatin [Chemicon], and 1X Phos-stop [Sigma]), and eluted in 2X sample buffer.

An immunoprecipitation was performed to demonstrate the dimerization of the Borealin-$2^{1–216}$-GCN4 construct. Borealin-$2^{1–216}$-GCN4-3XFLAG, Borealin-$2^{1–216}$-GCN4-GFP, Borealin-$2^{1–216}$-GFP, and GFP were expressed via the in vitro transcription and translation (TNT) system (Promega). Reticulocyte lysates containing Borealin-$2^{1–216}$-GCN4-3XFLAG were incubated with equal volumes of lysates containing either Borealin-$2^{1–216}$-GCN4-GFP, Borealin-$2^{1–216}$-GFP, or GFP for 1 h on ice to promote binding. Borealin-$2^{1–216}$-GCN4-3XFLAG, and its interactors were then captured by incubation with GFP-Trap Magnetic Agarose beads (Chromotek). GFP-Trap beads were then washed five times with wash buffer (20 mM HEPES, pH 7.7, 500 mM NaCl, 0.5 mM TCEP, 0.01% NP-40), and proteins were eluted with 2X sample buffer.

Equilibrium binding assay

A supernatant depletion binding assay was used (Lee *et al.*, 2000; Pollard, 2010) to determine the binding affinity of the Borealin dimerization domain for the Sgo1 N-terminus. Increasing amounts of GST-Borealin-$2^{216–296}$-bound Glutathione Sepharose 4B resin were titrated into solutions containing 2 µM Sgo$1^{1–150}$-His_6-MBP in 20 mM HEPES, pH 7.9, 150 mM NaCl, 1 mM TCEP at a final volume of 70 µl and were incubated for 1 h at 4°C with end-over-end rotation to achieve equilibrium. The mixtures were then briefly spun at 10,000 × *g* to pellet the beads, and 5 µl of each supernatant was immediately removed and added to 4X sample buffer, boiled at 95°C for 5 min, separated by SDS–PAGE electrophoresis, stained with GelCode Blue (ThermoFisher Scientific), and imaged on an Odyssey scanner (Licor). A control sample of 100 µM GST beads and 2 µM Sgo$1^{1–150}$-His_6-MBP was included to determine nonspecific binding. The concentration of Sgo1 left in the supernatant was calculated by analysis with ImageStudio software (Licor). A binding curve was generated by plotting the fraction of Sgo$1^{1–150}$-His_6-MBP bound (1- [Sgo1 in supernatant]) for each concentration of GST-Borealin-$2^{216–296}$. From this curve, the binding affinity (K_d) was calculated by fitting with the following equation in Prism (GraphPad): Fraction Sgo1 bound = [GST-Borealin-$2^{216–296}$]/(K_d + [GST-Borealin-$2^{216–296}$]).

Western blots

Primary antibodies were diluted in Licor blocking solution/PBST with a final Tween-20 concentration of 0.1%, except for anti-phospho Aurora and anti-Histone H3S10ph, which had no Tween-20. The following antibodies and antibody dilutions were used: anti-INCENP (raised against C-terminal peptide CSNRHHLAVGYGLKY) (5.5 µg/ml), anti-Aurora B (Kelly *et al.*, 2007; 5 µg/ml), anti-Borealin-2 (Dasra A; Kelly *et al.*, 2007; 5 µg/ml), anti-Survivin (Tseng *et al.*, 2010; 12 µg/ml), anti-phospho Aurora (Phospho-Aurora A [Thr288]/Aurora B [Thr 232]/Aurora C [Thr198] 2914, Cell Signaling Technology; 1:200), anti-Histone H3S10ph (6G3, 9706, Cell Signaling Technology; 1:500), anti-Histone H3T3ph (2162-1, Epitomics; 1:10,000), anti-GFP (11814460001, Sigma Aldrich; 1:1000), anti-PP2A-C (05-421, Millipore; 1:1000), Sgo1 (Boyarchuk *et al.*, 2007; 1:250), and anti-alpha-tubulin (DM1, Sigma; 1:20,000). Secondary antibodies from Licor were used (Licor goat anti-Rabbit 800 nm and Licor goat anti-mouse 680 nm), as was the Licor imaging system to scan membranes.

Microscopy and fluorescence quantification

To immunostain kinetochores, *Xenopus* egg extract was fixed for 5 min by ~20-fold dilution in BRB80 + 20% glycerol + 0.5% Triton X-100 + 3.7% formaldehyde at room temperature. Fixed reactions were layered onto a cushion of BRB80 + 40% glycerol overlaying a poly-L-lysine–coated coverslip (No. 1) placed in a 24-well plate. Nuclei were adhered onto coverslips on plate holders for 15 min at 4000 rpm at 18°C in a centrifuge (Eppendorf 5810R). Cushions were washed with BRB80 and coverslips were postfixed in ice-cold methanol for 5 min, blocked with Abdil (TBS + 0.1% Tween20 + 2% BSA + 0.1% sodium azide) overnight at 4°C, and then incubated in primary at room temperature for 1.5 h unless otherwise noted. All washes and antibody dilutions were done with AbDil buffer. Nuclei were stained with Hoechst 33258 before being mounted in 80% glycerol + PBS medium. The following antibodies were used at the indicated dilutions: INCENP (Haase *et al.*, 2017) 1:500, Borealin-2 (Dasra A) 1:250 (Kelly *et al.*, 2007), BubR1 (a kind gift of Alexei Arnoutav; Boyarchuk *et al.*, 2007) 1:100, and GFP-Booster Alexa Fluor 488 (GB2AF488, Chromotek) 1:500.

All immunofluorescence was imaged with 0.2 µm step size using an Eclipse Ti (Nikon) composed of a Nikon Plan Apo ×100/1.45, oil immersion objective, a PlanApo ×40/0.95 objective, and a Hamamatsu Orca-Flash 4.0 camera. Images were captured and processed using NIS Elements AR 4.20.02 software (Nikon) and analyzed in Fiji ImageJ. The acquired Z-sections of 0.2 µm each were converted to a maximum projection using NIS Elements and Fiji. Kinetochore intensity was measured using Fiji by centering 9 × 9– and 13 × 13–pixel regions over individual kinetochores. Total fluorescence intensity was recorded from each region. To correct for background fluorescence, the difference in intensities between the two regions was determined, and then made proportionate to the smaller region. This background value was then subtracted from the smaller region to determine kinetochore intensity with background correction as previously reported (Hoffman *et al.*, 2001).

Quantification and statistical analysis

All analyses were performed with a minimum number of either 50 spindles or 96 kinetochores for each assay. Sample size was chosen to ensure a high (>90%) theoretical statistical power in order to generate reliable P values. All graphs and statistical analysis were prepared with GraphPad Prism. Fluorescence values from experimental conditions were compared with control conditions using an ordinary one-way ANOVA with Turkey's multiple comparison tests to determine significance. All graphs show the mean with error bars representing the SD unless otherwise indicated.

Protein sequence alignment and homology modeling

All protein sequences were aligned in the Jalview program (2.11.0; Waterhouse *et al.*, 2009) using the Clustal or ClustalOWS algorithm. Clustalx coloring was applied without threshold for conservation.

A homology model of the Borealin-2 dimerization domain was generated based on the average NMR structure of the human Borealin dimerization domain (Bourhis *et al.*, 2009; PDB ID: 2KDD) using Robetta (Park *et al.*, 2018), and further refined using Galaxy Refine (Ko *et al.*, 2012).

ACKNOWLEDGMENTS

We thank Michael Lichten for critical reading of the manuscript; Adeline Walsh for technical assistance; and Mary Dasso, Alexei Arnaoutov, and Michael Lichten for kindly providing reagents and equipment. This work was supported by the Intramural Research

Program of the National Institutes of Health through the Center for Cancer Research, National Cancer Institute.

REFERENCES

Abad MA, Ruppert JG, Buzuk L, Wear M, Zou J, Webb KM, Kelly DA, Voigt P, Rappsilber J, Earnshaw WC, Jeyaprakash AA (2019). Borealin–nucleosome interaction secures chromosome association of the chromosomal passenger complex. J Cell Biol 218, 3912–3925.

Andersen KR, Leksa NC, Schwartz TU (2013). Optimized *E. coli* expression strain LOBSTR eliminates common contaminants from His-tag purification. Proteins 81, 1857–1861.

Andersen SS, Ashford AJ, Tournebize R, Gavet O, Sobel A, Hyman AA, Karsenti E (1997). Mitotic chromatin regulates phosphorylation of Stathmin/Op18. Nature 389, 640–643.

Bekier ME, Mazur T, Rashid MS, Taylor WR (2015). Borealin dimerization mediates optimal CPC checkpoint function by enhancing localization to centromeres and kinetochores. Nat Commun 6, 6775.

Blower MD (2016). Centromeric transcription regulates Aurora-B localization and activation. Cell Rep 15, 1624–1633.

Bonner MK, Haase J, Swinderman J, Halas H, Miller Jenkins LM, Kelly AE (2019). Enrichment of Aurora B kinase at the inner kinetochore controls outer kinetochore assembly. J Cell Biol 218, 3237–3257.

Bourhis E, Lingel A, Phung Q, Fairbrother WJ, Cochran AG (2009). Phosphorylation of a borealin dimerization domain is required for proper chromosome segregation. Biochemistry 48, 6783–6793.

Boyarchuk Y, Salic A, Dasso M, Arnaoutov A (2007). Bub1 is essential for assembly of the functional inner centromere. 176, 919–928.

Broad AJ, DeLuca KF, DeLuca JG (2020). Aurora B kinase is recruited to multiple discrete kinetochore and centromere regions in human cells. J Cell Biol 219, 785.

Caldas GV, DeLuca KF, DeLuca JG (2013). KNL1 facilitates phosphorylation of outer kinetochore proteins by promoting Aurora B kinase activity. J Cell Biol 203, 957–969.

Campbell CS, Desai A (2013). Tension sensing by Aurora B kinase is independent of survivin-based centromere localization. Nature 497, 118–121.

Carmena M, Wheelock M, Funabiki H, Earnshaw WC (2012). The chromosomal passenger complex (CPC): from easy rider to the godfather of mitosis. Nat Rev Mol Cell Biol 13, 789–803.

Date D, Dreier MR, Borton MT, Bekier ME, Taylor WR (2012). Effects of phosphatase and proteasome inhibitors on Borealin phosphorylation and degradation. J Biochem 151, 361–369.

Du J, Kelly AE, Funabiki H, Patel DJ (2012). Structural basis for recognition of H3T3ph and Smac/DIABLO N-terminal peptides by human Survivin. Structure 20, 185–195.

Elowe S, Hümmer S, Uldschmid A, Li X, Nigg EA (2007). Tension-sensitive Plk1 phosphorylation on BubR1 regulates the stability of kinetochore microtubule interactions. Genes Dev 21, 2205–2219.

Eshleman HD, Morgan DO (2014). Sgo1 recruits PP2A to chromosomes to ensure sister chromatid bi-orientation during mitosis. J Cell Sci 127, 4974–4983.

Fink S, Turnbull K, Desai A, Campbell CS (2017). An engineered minimal chromosomal passenger complex reveals a role for INCENP/Sli15 spindle association in chromosome biorientation. J Cell Biol 123, jcb.201609123–923.

Fischböck-Halwachs J, Singh S, Potocnjak M, Hagemann G, Solis-Mezarino V, Woike S, Ghodgaonkar-Steger M, Weissmann F, Gallego LD, Rojas J, *et al.* (2019). The COMA complex interacts with Cse4 and positions Sli15/Ipl1 at the budding yeast inner kinetochore. Elife 8, 1075.

Foley EA, Kapoor TM (2013). Microtubule attachment and spindle assembly checkpoint signalling at the kinetochore. Nat Rev Mol Cell Biol 14, 25–37.

Foley EA, Maldonado M, Kapoor TM (2011). Formation of stable attachments between kinetochores and microtubules depends on the B56-PP2A phosphatase. Nat Cell Biol 13, 1265–1271.

Gadea BB, Ruderman JV (2006). Aurora B is required for mitotic chromatin-induced phosphorylation of Op18/Stathmin. Proc Natl Acad Sci USA 103, 4493–4498.

García-Rodríguez LJ, Kasciukovic T, Denninger V, Tanaka TU (2019). Aurora B-INCENP localization at centromeres/inner kinetochores is required for chromosome bi-orientation in budding yeast. Curr Biol 29, 1536–1544.e4.

Haase J, Bonner MK, Halas H, Kelly AE (2017). Distinct roles of the chromosomal passenger complex in the detection of and response to errors in kinetochore–microtubule attachment. Dev Cell 42, 640–654.e5.

Hadders MA, Hindriksen S, Truong MA, Mhaskar AN, Wopken JP, Vromans MJM, Lens SMA (2020). Untangling the contribution of Haspin and Bub1 to Aurora B function during mitosis. J Cell Biol 219, 253.

Hengeveld RCC, Vromans MJM, Vleugel M, Hadders MA, Lens SMA (2017). Inner centromere localization of the CPC maintains centromere cohesion and allows mitotic checkpoint silencing. Nat Commun 8, 15542.

Hindriksen S, Lens SMA, Hadders MA (2017). The ins and outs of Aurora B inner centromere localization. Front Cell Dev Biol 5, 112.

Hoffman DB, Pearson CG, Yen TJ, Howell BJ, Salmon ED (2001). Microtubule-dependent changes in assembly of microtubule motor proteins and mitotic spindle checkpoint proteins at PtK1 kinetochores. Mol Biol Cell 12, 1995–2009.

Jeyaprakash AA, Basquin C, Jayachandran U, Conti E (2011). Structural basis for the recognition of phosphorylated histone h3 by the survivin subunit of the chromosomal passenger complex. Structure 19, 1625–1634.

Jeyaprakash AA, Klein UR, Lindner D, Ebert J, Nigg EA, Conti E (2007). Structure of a Survivin–Borealin–INCENP core complex reveals how chromosomal passengers travel together. Cell 131, 271–285.

Kawashima SA, Yamagishi Y, Honda T, Ishiguro K-I, Watanabe Y (2010). Phosphorylation of H2A by Bub1 prevents chromosomal instability through localizing shugoshin. Science 327, 172–177.

Kelly AE, Ghenoiu C, Xue JZ, Zierhut C, Kimura H, Funabiki H (2010). Survivin reads phosphorylated histone H3 threonine 3 to activate the mitotic kinase Aurora B. Science 330, 235–239.

Kelly AE, Sampath SC, Maniar TA, Woo EM, Chait BT, Funabiki H (2007). Chromosomal enrichment and activation of the aurora B pathway are coupled to spatially regulate spindle assembly. Dev Cell 12, 31–43.

Ko J, Park H, Heo L, Seok C (2012). GalaxyWEB server for protein structure prediction and refinement. Nucleic Acids Res 40, W294–W297.

Lee WL, Bezanilla M, Pollard TD (2000). Fission yeast myosin-I, Myo1p, stimulates actin assembly by Arp2/3 complex and shares functions with WASp. J Cell Biol 151, 789–800.

Liang C, Zhang Z, Chen Q, Yan H, Zhang M, Zhou L, Xu J, Lu W, Wang F (2020). Centromere-localized Aurora B kinase is required for the fidelity of chromosome segregation. J Cell Biol 219, 8364.

Liu H, Jia L, Yu H (2013a). Phospho-H2A and cohesin specify distinct tension-regulated Sgo1 pools at kinetochores and inner centromeres. Curr Biol 23, 1927–1933.

Liu H, Qu Q, Warrington R, Rice A, Cheng N, Yu H (2015). Mitotic transcription installs Sgo1 at centromeres to coordinate chromosome segregation. Mol Cell 59, 426–436.

Liu H, Rankin S, Yu H (2013b). Phosphorylation-enabled binding of SGO1-PP2A to cohesin protects sororin and centromeric cohesion during mitosis. Nat Cell Biol 15, 40–49.

Liu X, Song Z, Huo Y, Zhang J, Zhu T, Wang J, Zhao X, Aikhionbare F, Zhang J, Duan H, *et al.* (2014). Chromatin protein HP1 interacts with the mitotic regulator borealin protein and specifies the centromere localization of the chromosomal passenger complex. J Biol Chem 289, 20638–20649.

Meppelink A, Kabeche L, Vromans MJM, Compton DA, Lens SMA (2015). Shugoshin-1 balances Aurora B kinase activity via PP2A to promote chromosome bi-orientation. Cell Rep 11, 508–515.

Musacchio A, Desai A (2017). A molecular view of kinetochore assembly and function. Biology (Basel) 6, 5.

Niedzialkowska E, Wang F, Porebski PJ, Minor W, Higgins JMG, Stukenberg PT (2012). Molecular basis for phosphospecific recognition of histone H3 tails by Survivin paralogues at inner centromeres. Mol Biol Cell 23, 1457–1466.

O'Shea EK, Klemm JD, Kim PS, Alber T (1991). X-ray structure of the GCN4 leucine zipper, a two-stranded, parallel coiled coil. Science 254, 539–544.

Park H, Kim DE, Ovchinnikov S, Baker D, DiMaio F (2018). Automatic structure prediction of oligomeric assemblies using Robetta in CASP12. Proteins 86(Suppl 1), 283–291.

Pollard TD (2010). A guide to simple and informative binding assays. Mol Biol Cell 21, 4061–4067.

Presler M, Van Itallie E, Klein AM, Kunz R, Coughlin ML, Peshkin L, Gygi SP, Wühr M, Kirschner MW (2017). Proteomics of phosphorylation and protein dynamics during fertilization and meiotic exit in the *Xenopus* egg. Proc Natl Acad Sci USA 114, E10838–E10847.

Rivera T, Losada A (2009). Shugoshin regulates cohesion by driving relocalization of PP2A in *Xenopus* extracts. Chromosoma 118, 223–233.

Rivera T, Ghenoiu C, Rodríguez-Corsino M, Mochida S, Funabiki H, Losada A (2012). *Xenopus* Shugoshin 2 regulates the spindle assembly pathway mediated by the chromosomal passenger complex. EMBO J 31, 1467–1479.

Sampath SC, Ohi R, Leismann O, Salic A, Pozniakovski A, Funabiki H (2004). The chromosomal passenger complex is required for chromatin-induced microtubule stabilization and spindle assembly. Cell 118, 187–202.

Saurin AT (2018). Kinase and phosphatase cross-talk at the kinetochore. Front Cell Dev Biol 6, 62.
Sessa F, Mapelli M, Ciferri C, Tarricone C, Areces LB, Schneider TR, Stukenberg PT, Musacchio A (2005). Mechanism of Aurora B activation by INCENP and inhibition by hesperadin. Mol Cell 18, 379–391.
Tanno Y, Kitajima TS, Honda T, Ando Y, Ishiguro K-I, Watanabe Y (2010). Phosphorylation of mammalian Sgo2 by Aurora B recruits PP2A and MCAK to centromeres. Genes Dev 24, 2169–2179.
Trivedi P, Zaytsev AV, Godzi M, Ataullakhanov FI, Grishchuk EL, Stukenberg PT (2019a). The binding of Borealin to microtubules underlies a tension independent kinetochore-microtubule error correction pathway. Nat Commun 10, 682.
Trivedi P, Palomba F, Niedzialkowska E, Digman MA, Gratton E, Stukenberg PT (2019b). The inner centromere is a biomolecular condensate scaffolded by the chromosomal passenger complex. Nat Cell Biol 21, 1127–1137.
Tseng BS, Tan L, Kapoor TM, Funabiki H (2010). Dual detection of chromosomes and microtubules by the chromosomal passenger complex drives spindle assembly. Dev Cell 18:903–912.
Tsukahara T, Tanno Y, Watanabe Y (2010). Phosphorylation of the CPC by Cdk1 promotes chromosome bi-orientation. Nature 467, 719–723.
Ubersax JA, Ferrell JE (2007). Mechanisms of specificity in protein phosphorylation. Nat Rev Mol Cell Biol 8, 530–541.
Vallardi G, Allan LA, Crozier L, Saurin AT (2019). Division of labour between PP2A-B56 isoforms at the centromere and kinetochore. Elife 8, 683.
Verzijlbergen KF, Nerusheva OO, Kelly D, Kerr A, Clift D, de Lima Alves F, Rappsilber J, Marston AL (2014). Shugoshin biases chromosomes for biorientation through condensin recruitment to the pericentromere. Elife 3, 248.
Wang E, Ballister ER, Lampson MA (2011). Aurora B dynamics at centromeres create a diffusion-based phosphorylation gradient. 194, 539–549.
Wang F, Dai J, Daum JR, Niedzialkowska E, Banerjee B, Stukenberg PT, Gorbsky GJ, Higgins JMG (2010). Histone H3 Thr-3 phosphorylation by Haspin positions Aurora B at centromeres in mitosis. Science 330, 231–235.
Waterhouse AM, Procter JB, Martin DMA, Clamp M, Barton GJ (2009). Jalview Version 2—a multiple sequence alignment editor and analysis workbench. Bioinformatics 25, 1189–1191.
Wheelock MS, Wynne DJ, Tseng BS, Funabiki H (2017). Dual recognition of chromatin and microtubules by INCENP is important for mitotic progression. J Cell Biol 216, 925–941.
Wühr M, Freeman RM, Presler M, Horb ME, Peshkin L, Gygi SP, Kirschner MW (2014). Deep proteomics of the *Xenopus laevis* egg using an mRNA-derived reference database. Curr Biol 24, 1467–1475.
Xu Z, Cetin B, Anger M, Cho U-S, Helmhart W, Nasmyth K, Xu W (2009). Structure and function of the PP2A–shugoshin interaction. Mol Cell 35, 426–441.
Yamagishi Y, Honda T, Tanno Y, Watanabe Y (2010). Two histone marks establish the inner centromere and chromosome bi-orientation. Science 330, 239–243.
Yue Z, Carvalho A, Xu Z, Yuan X, Cardinale S, Ribeiro S, Lai F, Ogawa H, Gudmundsdottir E, Gassmann R, *et al.* (2008). Deconstructing Survivin: comprehensive genetic analysis of Survivin function by conditional knockout in a vertebrate cell line. 183, 279–296.
Zaytsev AV, Segura-Peña D, Godzi M, Calderon A, Ballister ER, Stamatov R, Mayo AM, Peterson L, Black BE, Ataullakhanov FI, *et al.* (2016). Bistability of a coupled Aurora B kinase-phosphatase system in cell division. Elife 5, e10644.
Zhang X, Lan W, Ems-McClung SC, Stukenberg PT, Walczak CE (2007). Aurora B phosphorylates multiple sites on mitotic centromere-associated kinesin to spatially and temporally regulate its function. Mol Biol Cell 18, 3264–3276.